

Out-of-Distribution Detection using Neural Activation Prior

Weilin Wan, Weizhong Zhang, and Cheng Jin[†]

Fudan University, Shanghai, China

([†]) corresponding author

wlwan23@m.fudan.edu.cn

Abstract. Out-of-distribution detection (OOD) is a crucial technique for deploying machine learning models in the real world to handle the unseen scenarios. In this paper, we first propose a simple yet effective Neural Activation Prior (NAP) for OOD detection. Our neural activation prior is based on a key observation that, for a channel before the global pooling layer of a fully trained neural network, the probability of a few neurons being activated with a large response by an in-distribution (ID) sample is significantly higher than that by an OOD sample. An intuitive explanation is that for a model fully trained on ID dataset, each channel would play a role in detecting a certain pattern in the ID dataset, and a few neurons can be activated with a large response when the pattern is detected in an input sample. Then, a new scoring function based on this prior is proposed to highlight the role of these strongly activated neurons in OOD detection. Our approach is plug-and-play and does not lead to any performance degradation on ID data classification and requires no extra training or statistics from training or external datasets. Notice that previous methods primarily rely on post-global-pooling features of the neural networks, while the within-channel distribution information we leverage would be discarded by the global pooling operator. Consequently, our method is orthogonal to existing approaches and can be effectively combined with them in various applications. Experimental results show that our method achieves the state-of-the-art performance on CIFAR benchmark and ImageNet dataset, which demonstrates the power of the proposed prior. Finally, we extend our method to Transformers and the experimental findings indicate that NAP can also significantly enhance the performance of OOD detection on Transformers, thereby demonstrating the broad applicability of this prior knowledge.

Keywords: Out-of-Distribution Detection · Global Pooling Layer · Feature Activation Analysis

1 Introduction

Deep learning has developed rapidly in the last decade and become a crucial technique in various fields. However, neural networks would frequently make erroneous judgments in inference when encounter the data that differs greatly

from their training data, which is known as out-of-distribution (OOD) data. This challenge is growing more prevalent and is particularly vital in safety-critical areas such as autonomous driving [10, 17] and medical diagnosis [30], which urges the development of effective OOD detection methods.

In practice, OOD data exhibits large diversity and is difficult to identify [42]. Existing studies typically formulate OOD detection as a one-class classification task, utilizing prior knowledge. They [11, 24, 44] propose various priors, based on which they further design scoring functions to distinguish OOD samples from ID samples. For example, Hendrycks et al. [11] observed that OOD samples always exhibit lower maximum softmax probabilities, and accordingly proposed using the maximal softmax probability output by a neural network as an OOD indicator. Liu et al. [24] found that OOD samples usually have lower logits values, and based on this, an energy function was proposed for OOD detection. Drawing from these precedents, it's clear that existing methods largely rely on the introduction of certain priors. While some promising results highlight the effectiveness of these heuristics, a gap remains in meeting the practical requirements of real-world applications. Importantly, we note that the focus of these priors is narrowly concentrated on features and weights following global pooling, while the characteristics before the pooling layer are consistently ignored. Thus, we believe that finding and incorporating priors that can complement these existing focuses is essential, which will constitute the main contribution of our work.

In this study, we propose a novel prior, called **Neural Activation Prior** (NAP), for OOD detection. NAP characterizes our key observation that for channels before the global pooling layer in a fully trained neural network (illustrated to Figure 3a), a few neurons have a significantly high probability to show a larger response when activated by in-distribution (ID) samples compared to OOD samples. An intuitive explanation for NAP is that channels in a model fully trained on an ID dataset play a role in detecting certain patterns in the input samples from the ID dataset. When such patterns are detected, a few neurons can be activated [13], resulting in larger responses. These large responses usually occur when the input sample is ID data, but when the input is OOD data, such responses are rarely observed. This is because the pattern that the neuron focuses on is unlikely to be present in the OOD data. To verify our proposed prior, we employed DenseNet architecture [15] on CIFAR-10 [20] and Texture [5] datasets, analyzing mean and maximum within-channel activations before global pooling at the penultimate layer. Figure 1 clearly demonstrates that ID samples showing significantly higher maximal activation values than OOD samples at equal average activation levels. This is not unique to the 333rd channel but is observed across most channels.

It is worth noting that our proposed prior is orthogonal to that used in current OOD detection methods. In the OOD detection field, as shown in Figure 3a, existing methods [8, 11, 23, 24, 33, 34] mainly focus on the outputs and weights of the neural network after global pooling, and use them to design scoring functions for OOD detection. In contrast, the prior we proposed is focus within the channels of the penultimate layer before global pooling. Since the information carried in

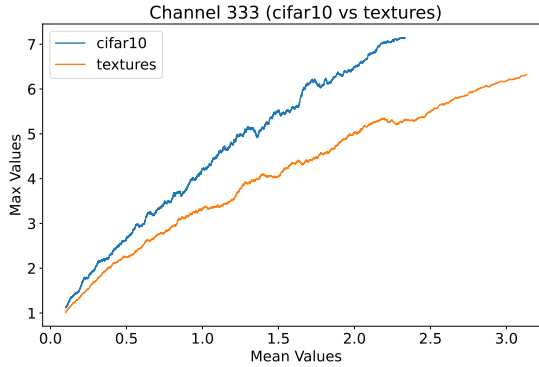


Fig. 1: Activation distribution difference between ID data and OOD data inside channel. This illustrates the difference in within-channel activation distribution between CIFAR-10 [20] (ID data) and the Texture [5] (OOD data) datasets. The horizontal axis represents the average activation value of the channel, while the vertical axis shows the maximal activation value of the channel. Interestingly, at the same mean activation levels, the ID data (CIFAR-10) show significantly higher maximum activation values within the channel compared to the OOD data (Texture). It's important to note that this pattern is **not unique** to the 333rd channel but is observed across most channels.

our prior can be easily lost during the global pooling process, this demonstrates that our NAP is essentially complementary to the priors used in current OOD detection studies. This property is verified in subsequent experiments Section 5.5 in this paper. To this end, we would like to emphasize that the contribution of this paper would lie in how much improvement we can achieve by integrating our method with existing approaches, rather than a direct comparison with existing methods in the field.

Furthermore, in this paper, we propose a simple yet effective scoring function for OOD detection based on our prior NAP. To be precise, our scoring function is based on the ratio of the maximal and averaged activation values within a channel. The rationale behind the scoring function can be understood from two primary perspectives: conceptual inspiration from the Signal-to-Noise (SNR) and empirical validation. On the conceptual front, inspired by the concept of SNR, we can consider the maximal activation value as signal strength, while the averaged activation value represents noise strength. Therefore, the ratio of the maximum to the average value can be used to measure the quality of information contained in the channel. On the empirical front, as shown in Figure 1, the ratio of the maximal and the averaged values for ID samples is significantly higher than that of OOD data. Regarding practical deployment, as previously mentioned, our scoring function complements and, when multiplied with existing metrics, improves OOD detection, as depicted in Figure 2. Also, it is noteworthy that this scoring function is a plug-and-play method, requiring no additional training,

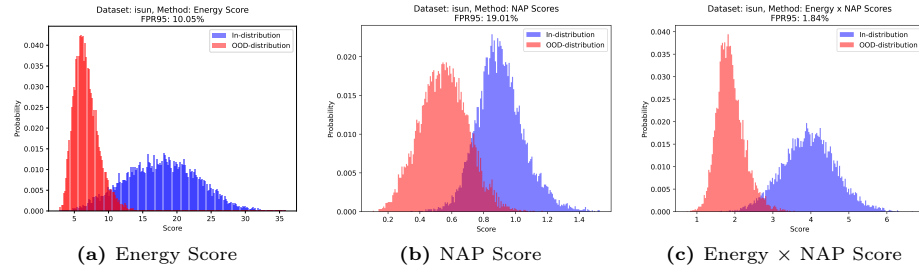


Fig. 2: Score Distribution Visualization Using DenseNet on CIFAR-10 (ID) and iSun (OOD) The integration of (a) Energy Score and (b) NAP Score through multiplication yields the (c) Energy \times NAP Score, demonstrating superior differentiation between ID and OOD datasets. The effectiveness of this approach is attributed to the orthogonal nature of the proposed NAP relative to conventional OOD detection methods exemplified by the Energy Score. This illustrates that a simple multiplicative combination with NAP enhances detection capability. Importantly, the objective here is not to outperform the Energy Score per se but to highlight the synergistic potential of NAP as a complementary enhancement to the Energy Score and similar methods.

extra data, or reliance on pre-calculated statistical data from the training set, which makes it broadly applicable.

Experimental results show that our method achieves state-of-the-art performance on CIFAR-10 [20], CIFAR-100 [20] and ImageNet datasets. Specifically, our method significantly reduces the false positive rate by 40.06% (from 15.05 to 9.02) on the CIFAR-10 dataset [20], a reduction of 37.89% (from 41.40 to 25.71) on the CIFAR-100 dataset [20], and a reduction of 16.26% (from 35.66 to 29.86) on the ImageNet dataset. The large drop in FPR95 highlights the effectiveness of our approach in different environments. The above experimental results demonstrate the power of our proposed prior. We believe that these findings will provide inspiration for other researchers and thus promote progress in the field of OOD detection.

Additionally, while convolutional neural networks (CNNs) are predominantly employed in OOD detection tasks, the advent of Transformer architectures [39] and their variants has showcased substantial efficacy across a diverse array of applications. Motivated by this, we extend our method to ensure compatibility with Transformer models. The empirical evidence obtained from our experiments affirms the robustness of our approach, demonstrating its adaptability to various architectural paradigms.

In summary, our contributions are as follows:

- We introduce the Neural Activation Prior (NAP), a novel contribution to OOD detection. Uniquely, NAP is orthogonal to priors utilized in existing methods, offering a distinct and complementary perspective that paves the way for advanced OOD detection research.
- Based on the proposed prior, we develop a simple yet effective OOD detection scoring function. It can be readily integrated with many existing OOD

detection techniques, enhancing their ability to balance OOD detection with ID accuracy.

- We demonstrate the state-of-the-art performance of our approach through extensive experiments across various datasets, including a reduction in FPR95 by up to 40.06%. These results underscore the method’s operational efficiency, simplicity of deployment, and overall efficacy.
- We extend the method to accommodate Transformer architectures. Experimental results are encouraging, validating the method’s efficacy across various architectural designs.

2 Related Work

2.1 OOD Detection

The OOD detection community has explored a variety of techniques to underscore the distinctions between ID and OOD samples. These methods encompass classification-based [3, 7, 12, 16, 23], density-based [1, 18, 19, 27, 29, 31, 47, 48], and distance-based approaches [4, 22, 25, 26, 35–37, 45], with classification-based techniques generally outperforming the other types [42]. In classification-based methods, the basic work of OOD detection starts with a simple and effective baseline: using the Maximum Softmax Probability (MSP) [12] to measure the probability that a certain sample is an ID sample. On this basis, early approaches [14, 23, 24] focused on developing enhanced OOD indicators derived from neural network outputs. In addition, some researchers have proposed strategies involving OOD sample generation [21] and gradient-based [23] techniques. Among these, certain post-hoc methods [8, 11, 23, 24, 33, 34, 44] are notable for their simplicity and because they do not necessitate changes in the training process or objectives. This feature is particularly valuable for implementing OOD detection in real production environments, where the additional cost and complexity associated with retraining would be unacceptable.

The MSP method, initially presented by Hendrycks et al. [11], was a formative step in post hoc OOD detection, using a neural network’s softmax output as a heuristic for distinguishing ID from OOD samples. Its straightforward application facilitated early adoption in OOD studies. Despite MSP’s influence, its limitations prompted further innovation, giving rise to the Energy method. This method, proposed by Liu et al. [24], refines the approach by assigning an energy score to network outputs, showing quantitative improvements over MSP with theoretical and empirical support. Advancements in post hoc OOD detection have led to diverse methodological branches stemming from MSP [12] and Energy [24] paradigms. LINe [2] innovates by reducing neuron-induced noise through the calculation of Shapley values. Yu et al. [44] distinguish ID from OOD data by identifying neural network blocks with optimal differentiation based on the norms of their features. DICE [34] improves discrimination by pruning weights in the fully connected layer according to the contribution units made during classification. On the other end of the spectrum, entirely computation-free post hoc methods such as ReAct [33] and ASH [8] have shown promise.

ReAct [33] investigates activations prior to the fully connected layer, applying rectification to suppress extreme activations that OOD data tend to trigger, thereby achieving refined detection outcomes. Similarly, ASH [8] prunes the activations inputted to the fully connected layer, but it achieves even more enhanced results compared to DICE [34] by its selective pruning strategy. In this paper, our comparison mainly focuses on post hoc methods, since our method also belongs to this category.

3 Neural Activation Prior

Our NAP is based on the following observation for OOD detection: for a channel located before the global pooling layer in a fully trained neural network, the likelihood that a small number of its neurons activated with a stronger response to an ID sample is significantly higher compared to an OOD sample. For the behavior in other layers of the neural network, refer to the discussion around Figure 5 in Section 5.5.

To formally describe this observation, we first define the concept of neural activation. Consider a trained classification neural network f , assuming it receives D -dimensional input x and outputs K -dimensional logits. That is $f : \mathbb{R}^D \rightarrow \mathbb{R}^K$. We concentrate on the activation tensor \mathbf{A} , located at the penultimate layer just before the global pooling operation, as illustrated in Figure 3a. Let the dimensions of \mathbf{A} be $C \times H \times W$, where C is the number of channels, and H and W are the spatial dimensions.

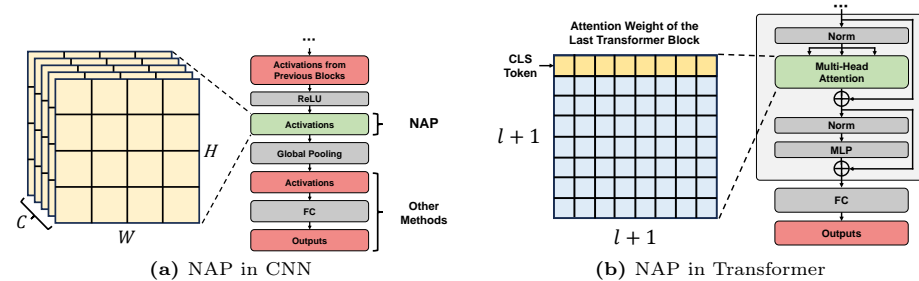


Fig. 3: Illustration identifying the focus zone of Neural Activation Prior (NAP) in classification neural networks. The figure highlights the specific position of NAP in the network: (a) For the CNN-based model, the activation value in the green part is the location of the NAP proposed in this article, which is before global pooling. (b) For the Transformer model, NAP is highlighted within the cls token’s attention weights in the last Transformer block, illustrating a targeted approach in contrast to most existing methods that focus on regions after global pooling.

Let \mathbf{A}_j represent the activation tensor of the j -th channel. We define two key statistical indicators of \mathbf{A}_j as follows:

– **Maximum Activation Value:**

$$\text{Max}(\mathbf{A}_j) = \max_{k,l} \mathbf{A}_{jkl},$$

where $\text{Max}(\mathbf{A}_j)$ is the maximum value among all elements in the activation vector \mathbf{A}_j . Notice that \mathbf{A}_{jkl} is processed by ReLU (as shown in Figure 3a), hence $\mathbf{A}_{jkl} \geq 0$.

– **Mean Activation Value:**

$$\text{Mean}(\mathbf{A}_j) = \frac{1}{h \times w} \sum_{k=1}^h \sum_{l=1}^w \mathbf{A}_{jkl},$$

where $\text{Mean}(\mathbf{A}_j)$ is the average of all activation values in the j -th channel.

Inspired by the concept of signal-to-noise ratio, we interpret $\text{Max}(\mathbf{A}_j)$ as the signal strength and $\text{Mean}(\mathbf{A}_j)$ as the noise strength. The ratio of these values can be viewed as an indicator of the quality of the activation vector \mathbf{A}_j . Note that we calculate this metric separately for each channel in the network, since different channels are usually used to detect different patterns. In the context of OOD detection, this quality measure can be used to assess whether the neural network recognizes the input sample — in other words, this measure can be used to judge whether a sample is within the training set distribution. As shown in Figure 1, this phenomenon is termed as the neural activation prior.

It is worth noting that our proposed prior is orthogonal to existing OOD detection methods. As illustrated in Figure 3a, existing methods mainly focus on the network output and weight of the penultimate layer after global pooling, and leverage them to design various scoring functions for OOD detection. In contrast, the prior we propose focuses on the channels of the penultimate layer before global pooling. Since the distribution information within these channels is inevitably lost during the global pooling process, our proposed prior is complementary to existing work.

Extension to Transformer Backbones. We observe that the classify (cls) token in the last block of Transformers can be effectively utilized as an analogue to the pooled activations used in CNNs for our method. Consequently, as illustrated in Figure 3b, we calculate NAP score by employing the attention vectors associated with the **cls** token from the final Transformer block. This approach mirrors our methodological framework in CNNs, facilitating a coherent extension across both architectures. The specifics of the scoring function for NAP, applicable to both CNNs and Transformers, will be further elucidated in Section 4.2.

4 OOD Detection with NAP

4.1 Basics

First, we will provide a brief overview of typical settings for OOD detection in image classification networks. Typically, classification networks use ID data,

that is, known training data sets, to train a classification model. Once training is completed, the model’s parameters are fixed, enabling it to effectively classify the categories within the training data set. In the testing phase, to identify OOD samples, researchers usually introduce a scoring function into the model. During the inference, samples mixed with OOD data are fed into this trained model. The model not only classifies each sample, but also uses a scoring function to generate a score for each one. This score is used to predict whether a sample belongs to an ID class in the training set, or an unknown OOD class.

4.2 Design of Scoring Function

Based on our prior proposed previously in Section 3, we propose a SNR-like scoring function. In our formulation, the mean activation value is interpreted as the noise intensity, while the maximal activation value is regarded as the signal strength. This conceptual framework leads to the following scoring function:

$$S_{NAP}(x; f) = \frac{1}{C} \sum_{j=1}^C \left(\frac{\text{Max}(\mathbf{A}_j)}{\text{Mean}(\mathbf{A}_j) + \epsilon} \right)^2,$$

where C represents the number of channels before global pooling. Note that a small constant $\epsilon > 0$ is added to ensure the numerical stability of the computation.

Scoring Function for Transformers. Consistent with the NAP score used in CNNs, we calculate the mean and maximum values of the attention that the cls token has towards all other tokens. The attention vector, denoted as A , has a dimensionality of $(l + 1)$, where l represents the sequence length. To maintain consistency with the NAP score calculation method used in CNN networks, we would typically divide the maximum value by the mean. However, we note that the mean value of the attention vector is always $1/(l + 1)$, rendering the denominator superfluous. Therefore, for simplicity, we design the NAP score function for Transformers as $S_{NAP}^{Former} = \text{Max}(A)$.

OOD Detection. The usage of scoring function $S_{NAP}(x; f)$ in this paper is similar to that of the energy score $-E(x; f)$. The energy scoring function $E(x; f)$ converts the logits output of the classification network f into a scalar $E(x; f) = -\log \sum_{i=1}^K e^{f_i(x)}$, where $f_i(x)$ is the logits output of category i . In OOD detection, the score employed for OOD detection is the negative energy score, $-E(x; f)$. Therefore, ID data is given a higher score, while OOD data is assigned a lower score.

We can combine these two scoring functions. In this paper, we adopt the weighted geometric mean method to combine them:

$$S_{NAP-E}(x; f, w) = -E(x; f)^w \cdot S_{NAP}(x; f)^{1-w}.$$

And when using $S_{NAP}(x; f)$ to enhance other energy score based OOD methods, we simply replace the function f in the above formula with the specific function of the corresponding method, such as f^{DICE} , f^{ReAct} , f^{ASH} , etc.

Discussion.

Table 1: Comparison with competitive post-hoc OOD detection method on CIFAR benchmarks. All values are percentages and are averaged over 6 OOD test datasets. Except for our proposed method, all other results are taken from [8]. The best result is highlighted in bold. Methods marked with an asterisk (*) are employed with the Energy Score [24]. Note: A. = Area Under the ROC Curve; F. = False Positive Rate at 95% True Positive Rate. Methods include MSP [11], ODIN [23], Mahalanobis distance [22], Energy [24], ReAct [33], DICE [34], and ASH [8].

Method	MSP	ODIN	Maha.	Energy	ReAct	DICE	ASH-B	ASH-S	NAP-E	NAP-A	NAP-R
CIFAR-10	F. ↓ 48.73	24.57	31.42	26.55	26.45	20.83	20.23	15.05	9.02	11.14	9.18
	A. ↑ 92.46	93.71	89.15	94.57	94.67	95.24	96.02	96.91	98.15	97.48	98.02
CIFAR-100	F. ↓ 80.13	58.14	55.37	68.45	62.27	49.72	48.73	41.40	32.61	35.40	25.71
	A. ↑ 74.36	84.49	82.73	81.19	84.47	87.23	88.04	90.02	92.84	91.21	93.18

- **Plug-and-Play Simplicity:** The scoring function we proposed is a plug-and-play approach that can be easily integrated into existing neural network architectures. It requires no additional training or external data and retains the model’s inherent classification capabilities. These properties make it practical and suitable for a variety of applications.
- **Orthogonal to Existing Approaches:** Based on our proposed priors, the scoring function we design is orthogonal to existing methods. As shown in Figure 1, the value ranges of the within-channel activation mean values of ID samples and OOD samples overlap. This puts existing methods into trouble when distinguishing between ID and OOD samples with close means values. Based on the prior we proposed, this kind of dilemma can be solved naturally, which illustrates the power of our proposed priors to provide new perspectives for identifying OOD data.

5 Experiments

5.1 Evaluation on CIFAR Benchmarks

Implementation Details. In our experiments, consistent with recent studies [8,33,34], we utilized 10,000 test images from both CIFAR-10 [20] and CIFAR-100 [20] as ID data. To gauge the performance of the model, six widely-used OOD datasets were employed as benchmarks. These datasets include SVHN [28], Textures [5], iSUN [41], LSUN-Crop [43], LSUN-Resize [43], and Places365 [46]. As for pre-trained model, we employed DenseNet [15], and we follow the training setting of DenseNet introduced in [34]. In terms of method implementation details, it’s noted that the value of ϵ in our scoring functions is consistently set to 1.0 for numerical stability. We experimented with three distinct implementations. The **NAP-E** represents the weighted geometric mean of S_{NAP} and $-E$, while **NAP-A** and **NAP-R** represent the weighted geometric mean of S_{NAP} with $-E(x; f^{ASH})$ and $-E(x; f^{ReAct})$, respectively. For experiments conducted on CIFAR-10, the threshold w was set to 0.4 for **NAP-E**, 0.5 for **NAP-A**,

Table 2: OOD detection results on ImageNet-1k [6]. All values are percentages. Except for our proposed method, all other results are taken from [8]. Methods marked with an asterisk (*) are employed with the **Energy** Score [24].

Method	OOD Datasets								Average	
	iNat. [38]		SUN [40]		Places [46]		Textures [5]			
	FPR95	AUROC	FPR95	AUROC	FPR95	AUROC	FPR95	AUROC		
MSP [11]	64.29	85.32	77.02	77.10	79.23	76.27	73.51	77.30	73.51	
ODIN [23]	55.39	87.62	54.07	85.88	57.36	84.71	49.96	85.03	54.20	
Maha. [22]	62.11	81.00	47.82	86.33	52.09	83.63	92.38	33.06	63.60	
Energy [24]	59.50	88.91	62.65	84.50	69.37	81.19	58.05	85.03	62.39	
ReAct* [33]	42.40	91.53	47.69	88.16	51.56	86.64	38.42	91.53	45.02	
DICE* [34]	43.09	90.83	38.69	90.46	53.11	85.81	32.80	91.30	41.92	
ASH-B* [8]	31.46	94.28	38.45	91.61	51.80	87.56	20.92	95.07	35.66	
ASH-S* [8]	39.10	91.94	43.62	90.02	58.84	84.73	13.12	97.10	38.67	
NAP-E	29.90	94.47	39.69	90.46	55.17	85.15	11.74	97.28	34.12	
NAP-A	26.26	95.10	32.89	92.77	48.69	87.92	11.60	97.32	29.86	
NAP-R	24.58	95.55	38.47	91.12	53.32	86.24	9.57	97.60	31.49	
									92.63	

and 0.4 for **NAP-R**. For CIFAR-100, the w was set to 0.4 for **NAP-E**, 0.6 for **NAP-A**, and 0.5 for **NAP-R**.

Comparison. For comparison, we adopted recent post-hoc OOD detection methods: MSP [11], ODIN [23], Mahalanobis distance [22], Energy [24], ReAct [33], DICE [34], and ASH [8].

Experimental Results. Table 1 shows the comparison of NAP with other post hoc OOD detection methods on the CIFAR-10 and CIFAR-100 benchmarks. As shown in the table, our method significantly outperforms all other methods on the CIFAR-10 and CIFAR-100 datasets, achieving state-of-the-art performance. In CIFAR-10, **NAP-E** reduces FPR95 by 40.06% (from 15.05 to 9.02) compared to the previous best method. In CIFAR-100, **NAP-R** reduces FPR95 by 37.89% (from 41.40 to 25.71) compared to the previous best method. What is impressive is that the implementation of **NAP-E** is extremely simple and does not cause any degradation in ID data classification accuracy. This enables **NAP-E** to achieve the optimal pareto front among existing methods, where relevant results can be seen in Section 5.4. The Above results demonstrate the effectiveness of our method and the power of NAP in OOD detection.

5.2 Evaluation on ImageNet

Implementation Details. In real-world applications, models are confronted with high-resolution images spanning a diverse range of scenes and features. Evaluations on large-scale datasets can provide insights into the performance of models in practical deployments. Thus, in line with recent research [8, 33, 34], we conduct experiments with NAP on the expansive ImageNet-1k [6] dataset in this study. Four dataset subsets, with all overlapping categories with ImageNet-1k eliminated, were employed as OOD benchmarks. These OOD datasets comprise Textures [5], Places365 [46], iNaturalist [38], and SUN [40]. We used MobileNetV2 [32] architecture, which pre-trained on ImageNet-1k [6]. The architec-

ture and parameters remain unchanged during the OOD detection stage. Parallel to the experiments conducted on the CIFAR [20] benchmarks, we experimented with three distinct implementations. For parameter settings, w was set to 0.6 for **NAP-E**, 0.8 for **NAP-A**, and 0.8 for **NAP-R**.

Experimental Results. Table 2 shows the comparison results of NAP with other post-hoc OOD detection methods on the ImageNet-1k [6] benchmark. As shown in the table, our method outperforms all other methods on the ImageNet-1k dataset [6], achieving state-of-the-art performance. We have observed that our method brings significant performance improvements on the iNaturalist and Textures datasets, which is particularly notable. Intuitively, most of the pictures in the Textures [5] dataset are of a texture nature, so there is a small probability of obtaining a large response value. And while samples in iNaturalist have a relatively simple background, and the animals and plants in the foreground have certain semantic differences from the samples in ImageNet-1k, therefor, a sample in iNaturalist [38] is not likely to trigger large response values. The reason why existing methods do not perform well on this dataset may be due to their focus on activation values after global pooling. We speculate that although texture pictures cannot cause large activation values, they can excite small-amplitude noise on the entire feature map. Since large response values tend to only appear in a small area on the feature map, after global pooling, ID samples and texture class samples are likely to obtain similar average activation values. This may compromise the separability of the two types of samples, causing existing work to perform poorly on such samples.

5.3 Evaluation on Transformer

Following the experimental setup described in Section 5.2, we conduct experiments on the Vision Transformer [9] (ViT-B/16) using ImageNet-1k as the ID dataset. Energy [24] and MSP [11] were selected as baseline methodologies for this analysis. The study further explores the enhancement of these baseline methods through the integration of NAP, resulting in two variants: NAP-E and NAP-M. Comparative results detailed in Table 3 demonstrate that the NAP method

Table 3: OOD detection results on ViT-B/16 using ImageNet-1k as ID data. All values are percentages. Except for our proposed method, all other results are taken from [8]. The best result is highlighted in bold. Methods marked with an asterisk (*) are employed with the **Energy** Score [24].

Method	OOD Datasets								Average	
	iNat. [38]		SUN [40]		Places [46]		Textures [5]			
	FPR95	AUROC	FPR95	AUROC	FPR95	AUROC	FPR95	AUROC		
Energy [24]	64.08	79.24	72.77	70.25	74.30	68.44	58.46	79.30	67.40	74.31
NAP-E	60.97	80.77	64.05	77.34	69.34	73.30	45.04	86.93	59.85	79.58
MSP [11]	51.47	88.16	66.53	80.93	68.65	80.38	60.21	82.99	61.72	83.12
NAP-M	47.09	88.23	59.45	82.78	63.38	80.48	47.70	87.93	54.40	84.85

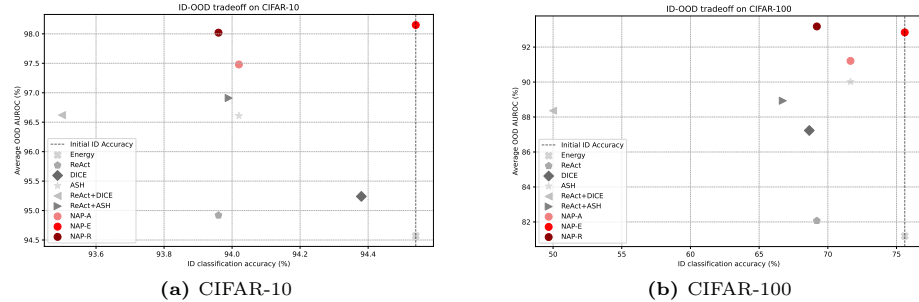


Fig. 4: Investigating the trade-offs between ID classification accuracy and OOD detection AUROC on CIFAR benchmarks [20] across various methods. All methods and experiments are implemented by us. Methods prefixed with 'NAP' are visually distinguished, highlighted in various shades of red in the figures.

substantially boosts the performance on Transformer architectures beyond the baselines, affirming the utility and versatility of NAP within such contexts.

5.4 Evaluation on Pareto Frontier of ID accuracy and OOD Detection Performance

Some existing methods negatively affect ID accuracy; however, we have found that integrating these methods with the NAP approach can mitigate or reduce this impact, achieving a more optimal balance. The NAP approach establishes an ideal equilibrium between ID classification accuracy and OOD detection efficacy (measured in AUROC), thereby positioning it favorably on the Pareto front for superior performance. This demonstrates our method's ability to enhance OOD detection without additional costs while maintaining the model's classification performance, as illustrated in Figures 4a and 4b using the CIFAR benchmark [20].

5.5 Ablation Studies

Comparison of S_{NAP} with Other Single Scoring Functions We evaluate S_{NAP} independently as a scoring function and compare them with two of the

Table 4: Comparison with other single OOD score on CIFAR benchmarks [20] and ImageNet-1k [6] dataset. CIFAR results are averaged across 6 different OOD tasks and ImageNet-1k results are averaged across 4 different OOD tasks.

Method	CIFAR-10		CIFAR-100		ImageNet-1k	
	FPR95	AUROC	FPR95	AUROC	FPR95	AUROC
MSP [11]	48.69	92.52	80.06	74.45	73.51	79.00
Energy [24]	26.59	94.63	68.29	81.23	62.39	84.91
S_{NAP}	26.57	92.45	54.91	85.86	49.91	83.07

Table 5: Ablation results on different w of **NAP-E** on CIFAR [20] benchmarks and ImageNet-1k [6] dataset.

w	CIFAR-10			CIFAR-100			ImageNet		
	FPR95	AUC	FPR95	AUC	FPR95	AUC	FPR95	AUC	FPR95
0.0	26.57	92.45	54.91	85.86	49.91	83.07	0.0	26.57	92.45
0.1	17.94	95.44	47.95	88.85	47.35	85.01	0.1	20.36	94.77
0.2	11.64	97.19	40.24	91.14	44.39	86.99	0.2	14.61	96.49
0.3	9.26	97.96	34.24	92.50	41.18	88.84	0.3	10.83	97.53
0.4	9.02	98.15	32.61	92.84	37.99	90.37	0.4	9.18	98.02
0.5	9.71	98.00	35.13	92.19	35.25	91.41	0.5	9.47	98.11
0.6	11.85	97.63	42.30	90.63	34.12	91.84	0.6	10.72	97.93
0.7	14.56	97.08	49.50	88.48	35.50	91.61	0.7	12.98	97.53
0.8	19.20	96.37	57.11	86.05	40.01	90.69	0.8	16.92	96.91
0.9	22.31	95.55	63.21	83.59	48.05	89.02	0.9	21.89	96.04
1.0	26.58	94.63	68.29	81.23	58.87	86.60	1.0	29.00	94.92

Table 6: Ablation results on different w of **NAP-R** on CIFAR [20] benchmarks and ImageNet-1k [6] dataset.

w	CIFAR-10			CIFAR-100			ImageNet		
	FPR95	AUC	FPR95	AUC	FPR95	AUC	FPR95	AUC	FPR95
0.0	26.57	92.45	54.91	85.86	49.91	83.07	0.0	26.57	92.45
0.1	20.36	94.77	49.80	87.75	48.59	84.21	0.1	20.36	94.77
0.2	14.61	96.49	44.03	89.58	46.82	85.49	0.2	14.61	96.49
0.3	10.83	97.53	36.81	91.21	44.88	86.92	0.3	10.83	97.53
0.4	9.18	98.02	29.66	92.47	42.43	88.44	0.4	9.18	98.02
0.5	9.47	98.11	25.71	93.18	39.42	89.96	0.5	9.47	98.11
0.6	10.72	97.93	26.83	93.15	36.02	91.33	0.6	10.72	97.93
0.7	12.98	97.53	32.02	92.13	33.03	92.32	0.7	12.98	97.53
0.8	16.92	96.91	43.99	89.86	31.49	92.63	0.8	16.92	96.91
0.9	21.89	96.04	57.95	86.37	34.38	91.78	0.9	21.89	96.04
1.0	29.00	94.92	69.94	82.07	49.90	88.75	1.0	29.00	94.92

most prevalent methods, MSP [11] and Energy [24], on both the CIFAR [20] benchmarks and the ImageNet-1k [6] dataset. As illustrated in Table 4, S_{NAP} alone outperforms MSP, while exhibiting varying degrees of advantages over Energy across different datasets. Considering the exceptional OOD detection capabilities of NAP-E as demonstrated in Tables 1 and 2, these results suggest that S_{NAP} is complementary to existing works. This complementarity allows for significant performance enhancements when S_{NAP} and existing methods are combined. It is important to clarify that while the results are presented in Table 4, the intention behind our method is not to surpass all existing methods in direct competition. As demonstrated by additional experimental outcomes, our method is orthogonal to others, representing our principal contribution.

Ablation on Different Parameter w . In Table 5 and 6, we show the various OOD detection performances of **NAP-E** and **NAP-R** on various datasets by varying the threshold w . It is important to note that our approach is essentially an ensemble approach. Generally, in ensemble approaches, it is advisable to avoid setting w extremely close to 0 or 1, to ensure effective contribution from all constituent models especially when the models are carefully chosen, diverse and useful. As an ensemble method, we provide the results of w over the entire interval [0,1] in Table 6 to show that our ensemble can always achieve significant improvements over the existing baseline and NAP. Note that these results are not provided to not to demonstrate the sensitivity of NAP to w . Furthermore, Table 6 show that near-optimal (if not optimal) performance is attainable around the mid-range values, especially near 0.5. As w is the only hyper parameter involved in our method, it allows us to employ a binary search to efficiently determine a desired value for w . The significant improvements in ensemble results verify that our method is orthogonal to existing energy-based approaches, which is one of the main contributions of this paper to the community. See the Appendix for more details about the performance impact of changes in w .

Does NAP Work Across All Network Layers? To assess the efficacy of the NAP across various layers within the DenseNet architecture, we conduct

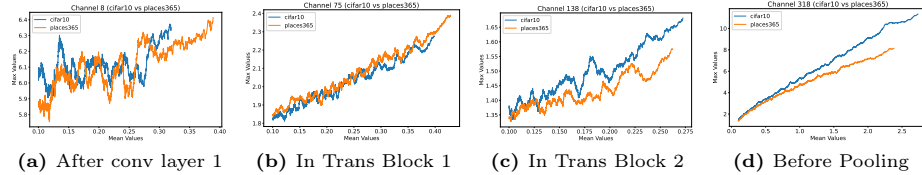


Fig. 5: Activation distribution at different positions within the DenseNet architecture [15] applied to CIFAR-10 [20] and Places365 datasets [46]. For this analysis, four specific locations within the network were chosen: (a) after the first convolution layer, (b) just before the pooling operation in the first transition block, (c) just before the pooling operation in the second transition block, and (d) right before the final global pooling layer. It is observed that with increasing depth, the separability between ID and OOD samples becomes more pronounced in the two-dimensional space defined by the maximum and average activation values.

a detailed examination of activation distributions utilizing the CIFAR-10 [20] and Places365 datasets [46]. Analysis focused on four pivotal points within the network: post-first convolutional layer, pre-pooling in the first and second transition blocks, and immediately preceding the final global pooling layer. Selected instances from the empirical findings are illustrated in Selected examples from our tests are shown in Figure 5, with more detailed visuals in the Appendix. From these figures, it's clear that the deeper the layer, the easier it is to tell apart ID and OOD samples based on the maximum and average activation values. In the network's early layers, neurons pick up basic features common to both ID and OOD samples, which explains why the lines cross in Figures 5a and 5b. Moving to deeper layers, neurons start capturing more complex, meaningful features. As seen in Figures 5c and 5d, ID samples with specific meanings trigger larger responses. This indicates that NAP works best closer to the end of the network, especially before the global pooling layer, highlighting its value in making models more reliable for OOD detection.

6 Conclusion

This paper proposes a novel Neural Activation Prior (NAP) for OOD detection in machine learning models. Our proposed prior is grounded on the observation that in a fully trained neural network, ID samples typically induce stronger activation responses in some neurons of a channel compared to OOD samples. This discovery led to our novel scoring function based on within-channel distribution. Its main advantage lies in its simplicity and easy integration. It necessitates neither additional training nor external data and does not compromise the classification performance on ID data. Experimental results on various datasets and architectures show that our method achieves state-of-the-art performance in OOD detection. This not only verifies the effectiveness of neural activation priors, but also demonstrates the potential of rethinking the way neural network features are utilized in OOD scenarios.

References

1. Abati, D., Porrello, A., Calderara, S., Cucchiara, R.: Latent space autoregression for novelty detection. In: Proceedings of the IEEE/CVF conference on computer vision and pattern recognition. pp. 481–490 (2019) [5](#)
2. Ahn, Y.H., Park, G.M., Kim, S.T.: Line: Out-of-distribution detection by leveraging important neurons. In: Proceedings of the IEEE/CVF Conference on Computer Vision and Pattern Recognition. pp. 19852–19862 (2023) [5](#)
3. Bendale, A., Boult, T.E.: Towards open set deep networks. In: Proceedings of the IEEE conference on computer vision and pattern recognition. pp. 1563–1572 (2016) [5](#)
4. Chen, X., Lan, X., Sun, F., Zheng, N.: A boundary based out-of-distribution classifier for generalized zero-shot learning. In: European conference on computer vision. pp. 572–588. Springer (2020) [5](#)
5. Cimpoi, M., Maji, S., Kokkinos, I., Mohamed, S., Vedaldi, A.: Describing textures in the wild. In: Proceedings of the IEEE conference on computer vision and pattern recognition. pp. 3606–3613 (2014) [2](#), [3](#), [9](#), [10](#), [11](#)
6. Deng, J., Dong, W., Socher, R., Li, L.J., Li, K., Fei-Fei, L.: Imagenet: A large-scale hierarchical image database. In: 2009 IEEE conference on computer vision and pattern recognition. pp. 248–255. Ieee (2009) [10](#), [11](#), [12](#), [13](#)
7. DeVries, T., Taylor, G.W.: Learning confidence for out-of-distribution detection in neural networks. *stat* **1050**, 13 (2018) [5](#)
8. Djurisic, A., Bozanic, N., Ashok, A., Liu, R.: Extremely simple activation shaping for out-of-distribution detection. In: The Eleventh International Conference on Learning Representations (2022) [2](#), [5](#), [6](#), [9](#), [10](#), [11](#)
9. Dosovitskiy, A., Beyer, L., Kolesnikov, A., Weissenborn, D., Zhai, X., Unterthiner, T., Dehghani, M., Minderer, M., Heigold, G., Gelly, S., et al.: An image is worth 16x16 words: Transformers for image recognition at scale. In: International Conference on Learning Representations (2020) [11](#)
10. Filos, A., Tigkas, P., McAllister, R., Rhinehart, N., Levine, S., Gal, Y.: Can autonomous vehicles identify, recover from, and adapt to distribution shifts? In: International Conference on Machine Learning. pp. 3145–3153. PMLR (2020) [2](#)
11. Hendrycks, D., Gimpel, K.: A baseline for detecting misclassified and out-of-distribution examples in neural networks. In: International Conference on Learning Representations (2016) [2](#), [5](#), [9](#), [10](#), [11](#), [12](#), [13](#)
12. Hendrycks, D., Gimpel, K.: A baseline for detecting misclassified and out-of-distribution examples in neural networks. In: International Conference on Learning Representations (2016) [5](#)
13. Hoefler, T., Alistarh, D., Ben-Nun, T., Dryden, N., Peste, A.: Sparsity in deep learning: Pruning and growth for efficient inference and training in neural networks. *The Journal of Machine Learning Research* **22**(1), 10882–11005 (2021) [2](#)
14. Hsu, Y.C., Shen, Y., Jin, H., Kira, Z.: Generalized odin: Detecting out-of-distribution image without learning from out-of-distribution data. In: Proceedings of the IEEE/CVF Conference on Computer Vision and Pattern Recognition. pp. 10951–10960 (2020) [5](#)
15. Huang, G., Liu, Z., Van Der Maaten, L., Weinberger, K.Q.: Densely connected convolutional networks. In: Proceedings of the IEEE conference on computer vision and pattern recognition. pp. 4700–4708 (2017) [2](#), [9](#), [14](#)
16. Huang, R., Li, Y.: Mos: Towards scaling out-of-distribution detection for large semantic space. In: Proceedings of the IEEE/CVF Conference on Computer Vision and Pattern Recognition. pp. 8710–8719 (2021) [5](#)

17. Janai, J., Güney, F., Behl, A., Geiger, A., et al.: Computer vision for autonomous vehicles: Problems, datasets and state of the art. *Foundations and Trends® in Computer Graphics and Vision* **12**(1–3), 1–308 (2020) [2](#)
18. Jiang, D., Sun, S., Yu, Y.: Revisiting flow generative models for out-of-distribution detection. In: *International Conference on Learning Representations* (2021) [5](#)
19. Kirichenko, P., Izmailov, P., Wilson, A.G.: Why normalizing flows fail to detect out-of-distribution data. *Advances in neural information processing systems* **33**, 20578–20589 (2020) [5](#)
20. Krizhevsky, A., Hinton, G., et al.: Learning multiple layers of features from tiny images (2009) [2](#), [3](#), [4](#), [9](#), [11](#), [12](#), [13](#), [14](#)
21. Lee, K., Lee, H., Lee, K., Shin, J.: Training confidence-calibrated classifiers for detecting out-of-distribution samples. In: *International Conference on Learning Representations* (2018) [5](#)
22. Lee, K., Lee, K., Lee, H., Shin, J.: A simple unified framework for detecting out-of-distribution samples and adversarial attacks. *Advances in neural information processing systems* **31** (2018) [5](#), [9](#), [10](#)
23. Liang, S., Li, Y., Srikant, R.: Enhancing the reliability of out-of-distribution image detection in neural networks. In: *International Conference on Learning Representations* (2018) [2](#), [5](#), [9](#), [10](#)
24. Liu, W., Wang, X., Owens, J., Li, Y.: Energy-based out-of-distribution detection. *Advances in neural information processing systems* **33**, 21464–21475 (2020) [2](#), [5](#), [9](#), [10](#), [11](#), [12](#), [13](#)
25. Lu, F., Zhu, K., Zhai, W., Zheng, K., Cao, Y.: Uncertainty-aware optimal transport for semantically coherent out-of-distribution detection. In: *Proceedings of the IEEE/CVF Conference on Computer Vision and Pattern Recognition*. pp. 3282–3291 (2023) [5](#)
26. Ming, Y., Sun, Y., Dia, O., Li, Y.: Cider: Exploiting hyperspherical embeddings for out-of-distribution detection. *arXiv preprint arXiv:2203.04450* **7**(10) (2022) [5](#)
27. Nalisnick, E., Matsukawa, A., Teh, Y.W., Gorur, D., Lakshminarayanan, B.: Do deep generative models know what they don't know? In: *International Conference on Learning Representations* (2018) [5](#)
28. Netzer, Y., Wang, T., Coates, A., Bissacco, A., Wu, B., Ng, A.Y.: Reading digits in natural images with unsupervised feature learning (2011) [9](#)
29. Pidhorskyi, S., Almohsen, R., Doretto, G.: Generative probabilistic novelty detection with adversarial autoencoders. *Advances in neural information processing systems* **31** (2018) [5](#)
30. Pooch, E.H., Ballester, P., Barros, R.C.: Can we trust deep learning based diagnosis? the impact of domain shift in chest radiograph classification. In: *Thoracic Image Analysis: Second International Workshop, TIA 2020, Held in Conjunction with MICCAI 2020, Lima, Peru, October 8, 2020, Proceedings 2*. pp. 74–83. Springer (2020) [2](#)
31. Sabokrou, M., Khalooei, M., Fathy, M., Adeli, E.: Adversarially learned one-class classifier for novelty detection. In: *Proceedings of the IEEE conference on computer vision and pattern recognition*. pp. 3379–3388 (2018) [5](#)
32. Sandler, M., Howard, A., Zhu, M., Zhmoginov, A., Chen, L.C.: Mobilenetv2: Inverted residuals and linear bottlenecks. In: *Proceedings of the IEEE conference on computer vision and pattern recognition*. pp. 4510–4520 (2018) [10](#)
33. Sun, Y., Guo, C., Li, Y.: React: Out-of-distribution detection with rectified activations. *Advances in Neural Information Processing Systems* **34**, 144–157 (2021) [2](#), [5](#), [6](#), [9](#), [10](#)

34. Sun, Y., Li, Y.: Dice: Leveraging sparsification for out-of-distribution detection. In: European Conference on Computer Vision. pp. 691–708. Springer (2022) [2](#), [5](#), [6](#), [9](#), [10](#)
35. Sun, Y., Ming, Y., Zhu, X., Li, Y.: Out-of-distribution detection with deep nearest neighbors. In: International Conference on Machine Learning. pp. 20827–20840. PMLR (2022) [5](#)
36. Techapanurak, E., Suganuma, M., Okatani, T.: Hyperparameter-free out-of-distribution detection using cosine similarity. In: Proceedings of the Asian conference on computer vision (2020) [5](#)
37. Van Amersfoort, J., Smith, L., Teh, Y.W., Gal, Y.: Uncertainty estimation using a single deep deterministic neural network. In: International conference on machine learning. pp. 9690–9700. PMLR (2020) [5](#)
38. Van Horn, G., Mac Aodha, O., Song, Y., Cui, Y., Sun, C., Shepard, A., Adam, H., Perona, P., Belongie, S.: The inaturalist species classification and detection dataset. In: Proceedings of the IEEE conference on computer vision and pattern recognition. pp. 8769–8778 (2018) [10](#), [11](#)
39. Vaswani, A., Shazeer, N., Parmar, N., Uszkoreit, J., Jones, L., Gomez, A.N., Kaiser, Ł., Polosukhin, I.: Attention is all you need. Advances in neural information processing systems **30** (2017) [4](#)
40. Xiao, J., Hays, J., Ehinger, K.A., Oliva, A., Torralba, A.: Sun database: Large-scale scene recognition from abbey to zoo. In: 2010 IEEE computer society conference on computer vision and pattern recognition. pp. 3485–3492. IEEE (2010) [10](#), [11](#)
41. Xu, P., Ehinger, K.A., Zhang, Y., Finkelstein, A., Kulkarni, S.R., Xiao, J.: Turkergaze: Crowdsourcing saliency with webcam based eye tracking. arXiv preprint arXiv:1504.06755 (2015) [9](#)
42. Yang, J., Zhou, K., Li, Y., Liu, Z.: Generalized out-of-distribution detection: A survey. arXiv preprint arXiv:2110.11334 (2021) [2](#), [5](#)
43. Yu, F., Seff, A., Zhang, Y., Song, S., Funkhouser, T., Xiao, J.: Lsun: Construction of a large-scale image dataset using deep learning with humans in the loop. arXiv preprint arXiv:1506.03365 (2015) [9](#)
44. Yu, Y., Shin, S., Lee, S., Jun, C., Lee, K.: Block selection method for using feature norm in out-of-distribution detection. In: Proceedings of the IEEE/CVF Conference on Computer Vision and Pattern Recognition. pp. 15701–15711 (2023) [2](#), [5](#)
45. Zaeemzadeh, A., Bisagno, N., Sambugaro, Z., Conci, N., Rahnavard, N., Shah, M.: Out-of-distribution detection using union of 1-dimensional subspaces. In: Proceedings of the IEEE/CVF conference on Computer Vision and Pattern Recognition. pp. 9452–9461 (2021) [5](#)
46. Zhou, B., Lapedriza, A., Khosla, A., Oliva, A., Torralba, A.: Places: A 10 million image database for scene recognition. IEEE transactions on pattern analysis and machine intelligence **40**(6), 1452–1464 (2017) [9](#), [10](#), [11](#), [14](#)
47. Zisselman, E., Tamar, A.: Deep residual flow for out of distribution detection. In: Proceedings of the IEEE/CVF Conference on Computer Vision and Pattern Recognition. pp. 13994–14003 (2020) [5](#)
48. Zong, B., Song, Q., Min, M.R., Cheng, W., Lumezanu, C., Cho, D., Chen, H.: Deep autoencoding gaussian mixture model for unsupervised anomaly detection. In: International conference on learning representations (2018) [5](#)